



Numerical Investigation of Interfacial Stress Distribution in Adhesive-Bonded Joints for Different Adhesive Materials

Somnath Somadder ^{*}, Palash Das, Md. Ashraful Islam, Md. Abdul Hasib

Department of Mechanical Engineering, Khulna University of Engineering & Technology, Khulna, Bangladesh

^{*}E-mail address: somnath@me.kuet.ac.bd ^{*}, palashdas1605002@gmail.com ^b, ashraf.bitr@gmail.com ^c,
ahasib@me.kuet.ac.bd ^d

ORCID numbers of authors:

0000-0001-6389-234X ^{*}, 0000-0003-0137-8390, 0000-0001-8864-9645, 0000-0002-2915-7840

Received date: 18.05.2022

Accepted date: 04.08.2022

Abstract

The widespread use of adhesive bonded connections has been used in a range of technical fields. In this paper, the interfacial stress distribution of adhesive bonded joint is presented. When determining whether or not a structure is dependable for use in operation, the stresses that act along the bond line of an adhesively bonded lap joint are of the utmost importance. The purpose of this study is to develop finite element solutions that are able to anticipate shear and peel stresses using the theory of elasticity as their foundation. The effect of adhesive properties on stress distribution is investigated by using different adhesive materials. By analysing five different adhesive materials it is concluded that 'adhesive I' is more reliable for operation.

Keywords: Adhesive bonded joints, Interfacial stress, Finite element solution, Adhesive materials.

1. Introduction

The adhesive joints have found widespread application in a variety of engineering fields, in particular those fields in which proper bonding is essential to the structural integrity of the building. There are many different kinds of bonded joints, the most popular of which are the single lap joint, the double lap joint, and the scarf junction. The single lap joint is the joint that has received the most research due to its straightforward geometry and ease of preparation. The scarf joint is superior to all the other types of joints because it has the highest possible strength in the same bonding zone. The geometric discontinuity that might occur in lap joints is removed in scarf joints, which results in a reduction in the amount of stress concentration [1]. Adhesive bonded joint refers to the joint formed when two or more materials are adhered together. When two dissimilar materials are adhered together, the interface region is subjected to significant stress. On adhesively bonded joints, researchers have employed analytical, computational, and experimental methodologies. The numerical investigation of interfacial stress distribution in adhesive-bonded joints for different adhesive materials is important to select the proper adhesive for the joint. There are numerous accessible analytical models for adhesively glued joints. T. S. Methfessel and W. Becker devised a generalized model for forecasting stress distributions in thick adhesive junctions [2]. Somnath Somadder and Md. Shahidul Islam evaluated the effect of adhesive layer thickness and slant angle on piezoelectric bonded joints



by utilizing the commercial 3-D finite element software ABAQUS [3]. An analytical solution for adhesive bonded joints was proposed by Tsai et al. [4]. Mokhtari et al. conducted a computational analysis to determine the effects of material characteristics on the stress distributions in the composite double lap joint [5]. Moya-Sanz et al. built a two-dimensional numerical model in Abaqus/Standard using the cohesive zone model to study the effect of geometry on the system. It is widely acknowledged that the Moya-Sanz model is one of the most significant contributions to the field of adhesive bonded joint research [6].

Experiments on adhesively bonded joints' strength and failure loads have been carried out by a number of researchers in order to gain this information. Experiments were done in order to ascertain the failure load of a single-lap joint by Ozel et al. [7]. Fatigue analysis of fastening joints of sheet materials using finite element method was carried out by Xiaocong He et al. [8]. A new material model for 2D finite element analysis of adhesive bonded joints was developed by Libin Zhao et al. [9]. Numerical investigation of mono and bi- adhesive aluminum joints was carried out by I. Pires et al. [10]. Stress analysis of an adhesively bonded single lap joint was carried out by René Quispe Rodríguez et al. [11]. Dynamic analysis of a single lap jointed cantilever beams was investigated by Xiaocong He [12]. Mechanical behavior of adhesive joints was investigated numerically by Xiaocong He and Yue Zhang [13]. Three dimensional analysis of bi-adhesively bonded double lap joint using finite element method was investigated by H. Ozer and O. Oz [14]. An analytical model for predicting the stress distributions within single-lap adhesively bonded beams was developed by Xiaocong He and Yuqi Wang [15]. In this study the interfacial stress distribution of adhesive bonded joints for various adhesive materials have been evaluated. A numerical analysis was carried out to compare and contrast among the adhesives. ABAQUS CAE tool was used in finite element analysis.

2. Mathematical Modeling

The adherends are modeled as Bernoulli-Euler beam models with axial and bending deformation modes. The formulation of this element can be found as follows:

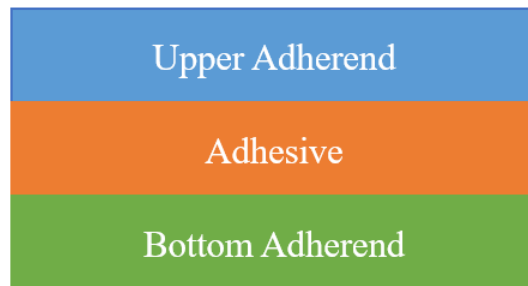


Fig. 1. General model of an adhesive bonded joint

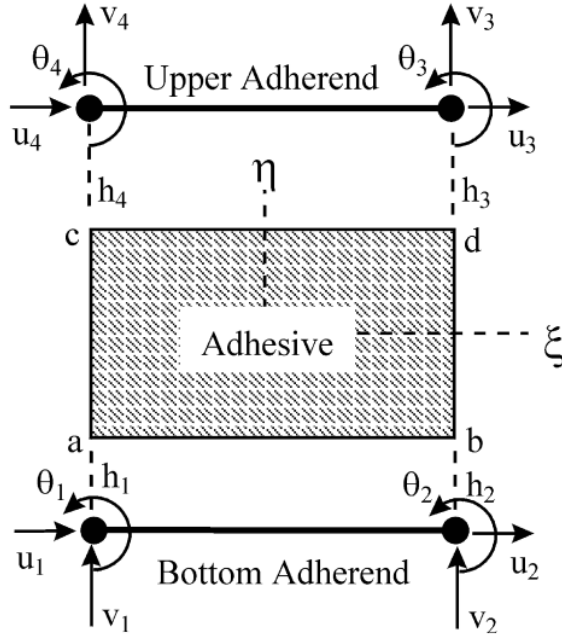


Fig. 2. 2D finite element model [16]

The axial and transverse displacement are approximated with the application of the following interpolation function.

$$u = \sum_i^2 \psi_i u_i \quad (1)$$

$$v = \sum_i^4 \phi_i s_i$$

Here, u_i and s_i are nodal displacements; ψ_i is linear Lagrange interpolation function and ϕ_i is cubic Hermit interpolation function. Substituting Eq. (1) into the virtual work expression,

$$[K_{adher}(\{\Delta\})]\{\Delta\} = \{F\} \quad (2)$$

Here, $\{\Delta\}$ is the nodal displacement vector, $K_{adher}(\{\Delta\})$ is the stiffness matrix, $\{F\}$ is the nodal force vector.

Within the framework of the finite element discretization, the coordinates of any point within the adhesive can be described as a function of the element's nodal coordinates.

$$\{x\} = \sum N_i x_i \quad (3)$$

Here, x is the coordinate of a generic point. This leads to the following formula for the displacement of the bottom adherend,

$$\{u_{adhes}\} = [N_i]_{adhes} \{u_i\}_{adhes} \quad (4)$$

In adhesive-adherend interactions, the continuity of displacement is given by,

$$\{u_{adhes}\}_{ab} = [N_{iab}]_{adhes} \{u_i\}_{adhes} = \{u_{adher}\}_b = [N_i]_{adher} \{u_i\}_{adher_b} \quad (5)$$

$$\{u_{adhes}\}_{cd} = [N_{icd}]_{adhes} \{u_i\}_{adhes} = \{u_{adher}\}_u = [N_i]_{adher} \{u_i\}_{adher_u} \quad (6)$$

where $[N_{iab}]_{adhes}$ and $[N_{icd}]_{adhes}$ are the interpolation functions for the adhesive evaluated at the ab and cd interfaces, respectively. The displacements in the adhesive layer are derived as a function of the nodal displacement of the adherends by using these formulas.

$$\{u_{adhes}\} = [N'_i] \{u\}_{adher} \quad (7)$$

where $[N'_i]$ is the interpolations functions of the displacements in the adhesive layer with respect to the adherend nodal displacements.

The constitutive law of the adhesive can be expressed as,

$$D = \frac{E}{(1+\nu)(1-2\nu)} \begin{bmatrix} 1-\nu & \nu & 0 \\ \nu & 1-\nu & 0 \\ 0 & 0 & \frac{1-2\nu}{2} \end{bmatrix} \quad (8)$$

where E is the elastic modulus and ν the Poisson ratio

The model of the finite elements can be obtained by doing the following:

$$[K_{adhes}(\{\Delta\})] \{\Delta\} = \{F\} \quad (9)$$

The sum of the stiffness matrices of the adherend and the adhesive constitutes the model of the adherend-adhesive system.

$$[K_{adher} + K_{adhes}] \{\Delta\} = [K] \{\Delta\} \{F\} \quad (10)$$

Eq. (10) can be written as,

$$[K_L + K_{NL}] \{U\} = \{F\} \quad (11)$$

3. Finite Element Modeling

The development of the finite element model is accomplished with the help of the ABAQUS finite element program. The simulation was carried out by taking into account adhesive bonds that were stressed by mechanical loads. For the purpose of stress analysis, the general static step is utilized.

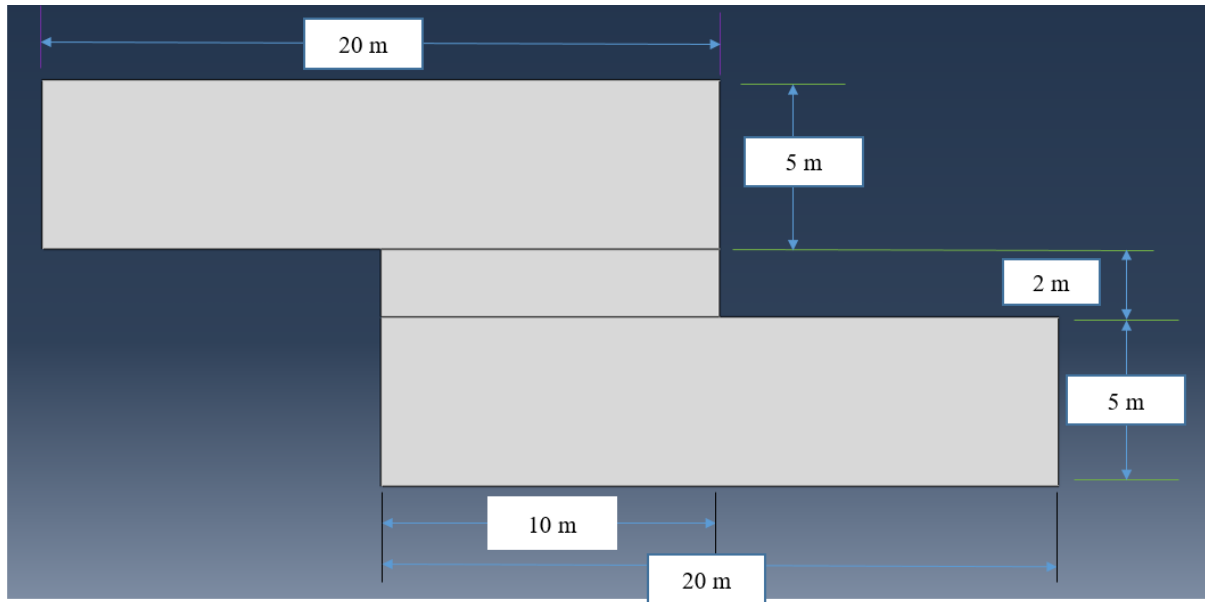


Fig. 3. Physical representation of the model

Within the scope of this study, three rectangular bars have been taken into consideration for the examination. Figure 3 shows that the upper and lower adherends each measure 20 meters in length and 5 meters across. This dimensions are taken as practical implementation of industrial applications such as electronic packaging and building constructions. The adhesive layer, which is 10 meters in length and 2 meters in width.

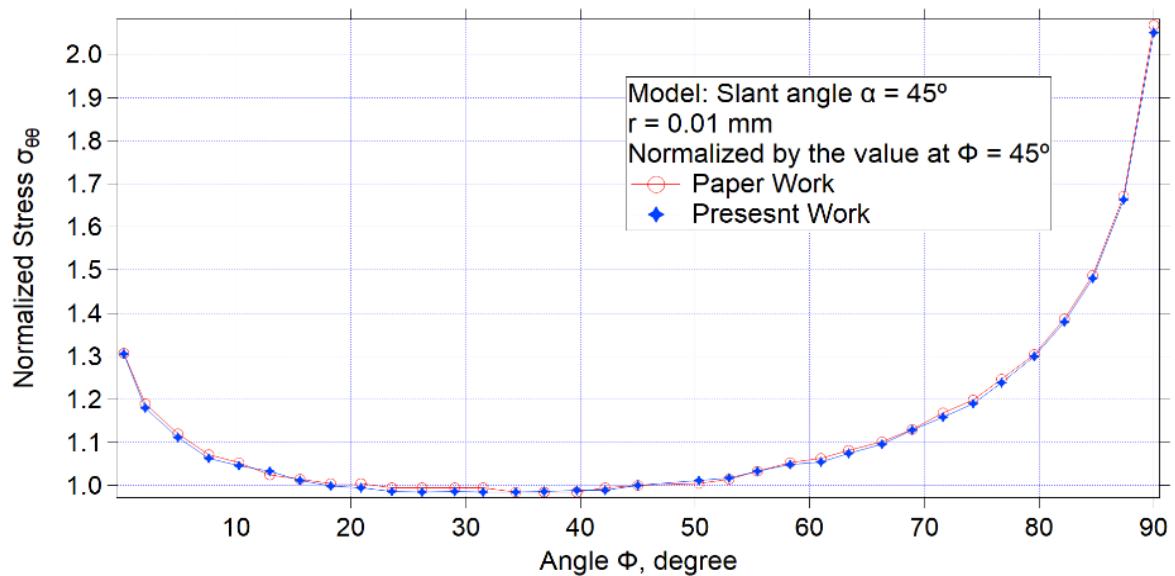


Fig. 4. Comparison of present analysis with reference paper analysis for the validation of research work

Figure 4 indicates that the results obtained in the present analysis are in good agreement with the results of Hideo Koguchi and Joviano Antonio da Costa [17] where the maximum error percentage is less than 1%.

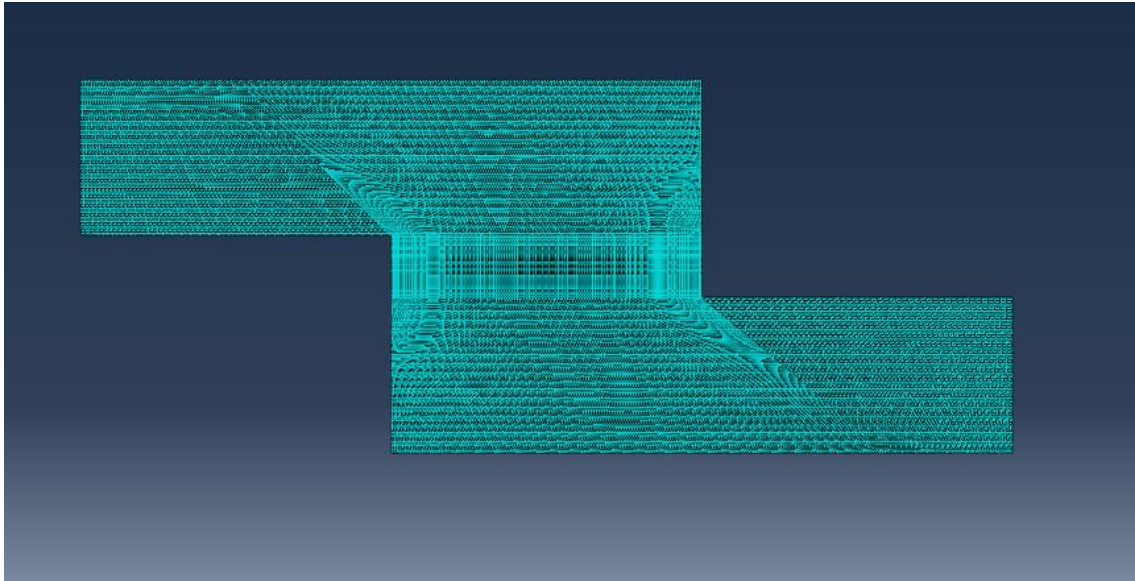


Fig. 5. Mesh of the model

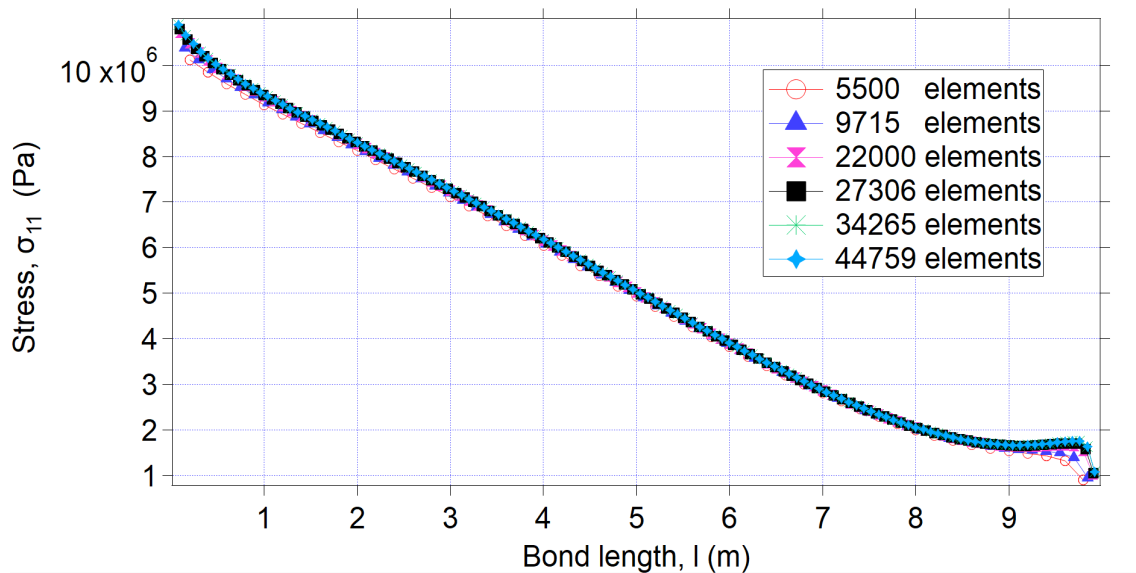


Fig. 6. Mesh sensitivity analysis of the model

Figure 5 indicates the mesh of the model. A bias has been introduced near the interface region, which has resulted in a greater concentration of elements in that region compared to those in the other regions. Because this is a two-dimensional FEM analysis, the plane stress condition is taken into account. The CPS4R mesh element type, which is a 4-node biquadratic, reduced integration element, is the one that is utilized here. Following the completion of a mesh sensitivity study as shown in figure 6, 34265 elements will be utilized in the subsequent analysis.

3.1. Material properties

Titanium is employed as the lower adherend material, and aluminum is used for the higher adherend material in this instance.

Table 1. The characteristics of the materials that were used for the examination [18].

Material	$E(GPa)$	ν
Aluminum (1050A-H9)	72	0.33
Titanium	108	0.30
Adhesive I	0.01	0.32
Adhesive II	0.1	0.33
Adhesive III	1	0.35
Adhesive IV	2	0.36
Adhesive V	5	0.40

3.2. Boundary condition

In this investigation, a mechanical force of 1 MPa is exerted on the right side of the lower adherend, while the left side of the higher adherend remains fixed. After generating the pieces and assigning material qualities the parts are joined together. The problem was effectively solved by developing a static step, putting in place appropriate boundary and loading conditions, and so on.

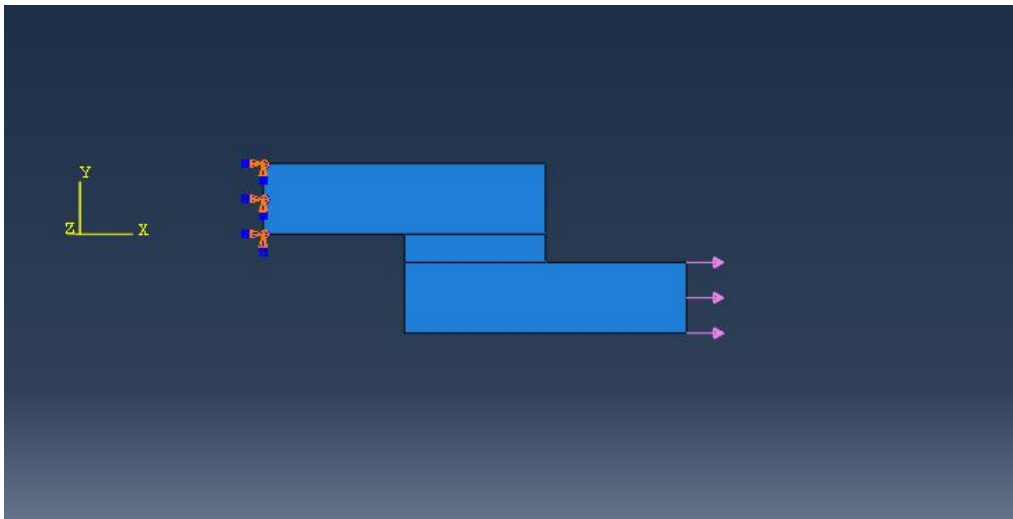


Fig. 7. Model showing boundary condition of the analysis

4. Result and Discussion

In order to analyze the stress and displacement characteristics of each simulated result, all of the results are plotted against the bond line. Please find below a presentation of the graphical illustrations.

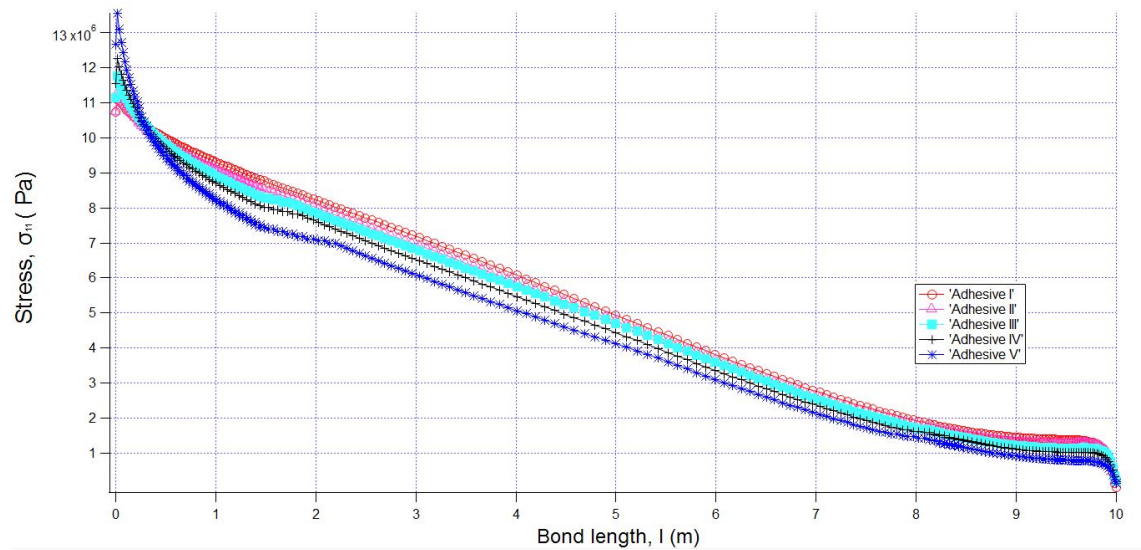


Fig. 8. Variation of σ_{11} along the bond line of the adhesive bonded joint

The distribution of σ_{11} along the bond line of the adhesive bonded joint is depicted in Figure 8. Here σ_{11} represents the variation of normal stress distribution along the X direction. It can be seen from the figure that the amount of stress is the greatest for adhesive V and that it is the lowest for adhesive I. As a result, adhesive I need to be utilized to ensure reliable operation.

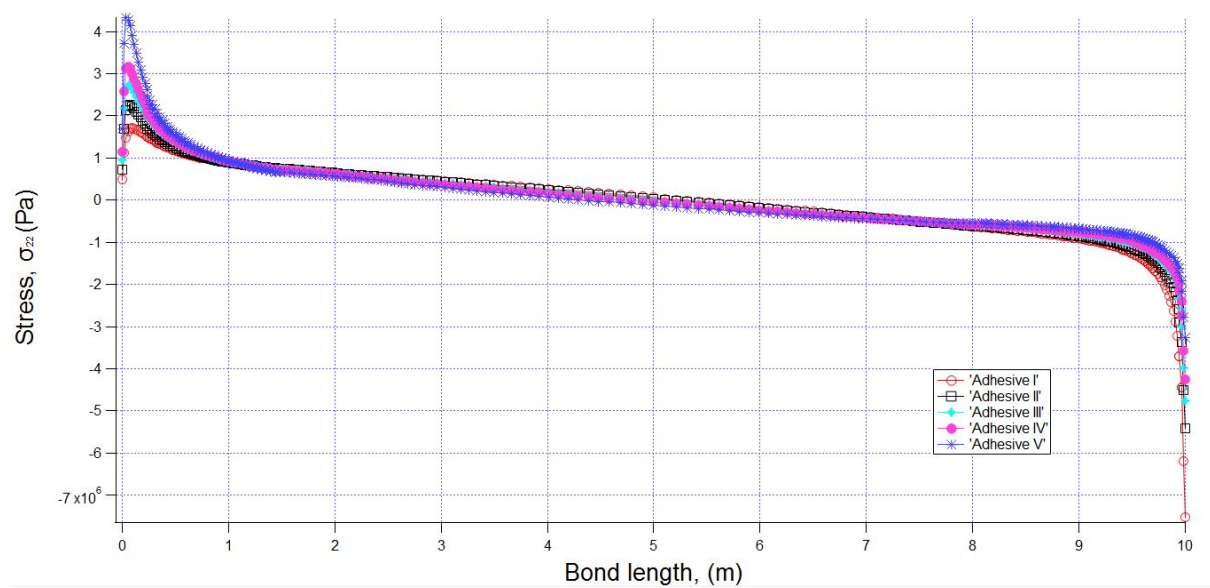


Fig. 9. Variation of σ_{22} along the bond line of the adhesive bonded joint

Figure 9 shows the distribution of σ_{22} along the bond line of the adhesive bonded joint. Here σ_{22} represents the variation of normal stress distribution along the Y direction. It can be seen from the figure that the amount of stress that is present is greater near the interface regions than it is in any of the other places. When it comes to the distribution of stress, adhesive V receives

the most while adhesive I receives the least. As a result, adhesive I should be used so that the operation can be trusted.

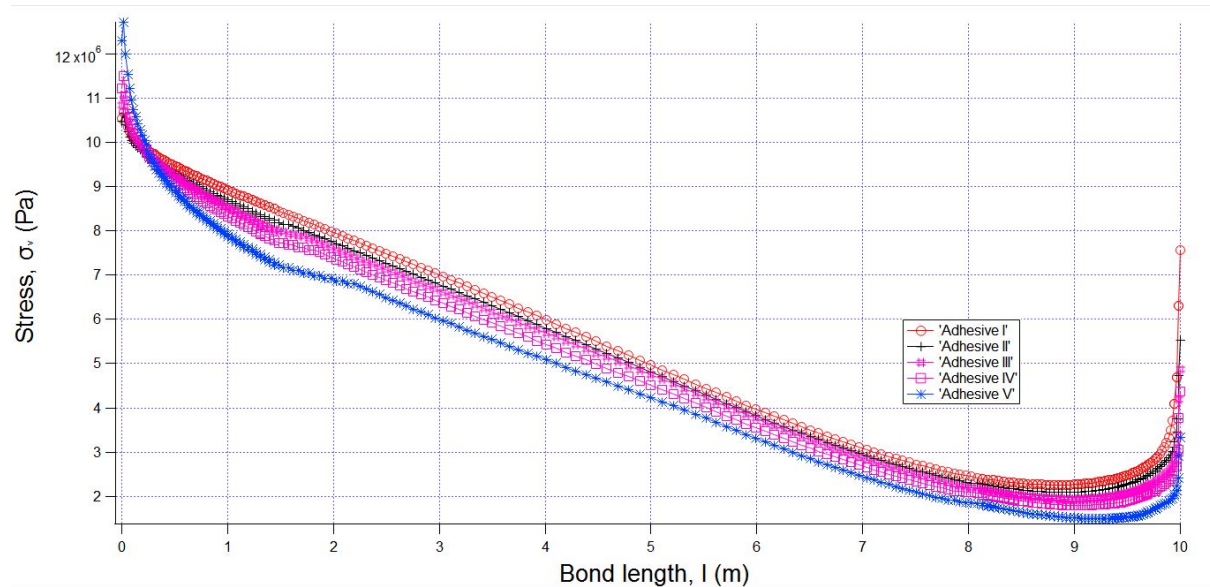


Fig. 10. Variation of Von Mises stress along the bond line of the adhesive bonded joint

The distribution of Von Mises stress along the bond line of the adhesive bonded joint is depicted in Figure 10. It can be seen from the figure that the amount of stress that is present is greater near the interface regions than it is in any of the other places. When it comes to the distribution of stress, adhesive V receives the most while adhesive I receives the least. As a result, adhesive I should be used so that the operation can be trusted.

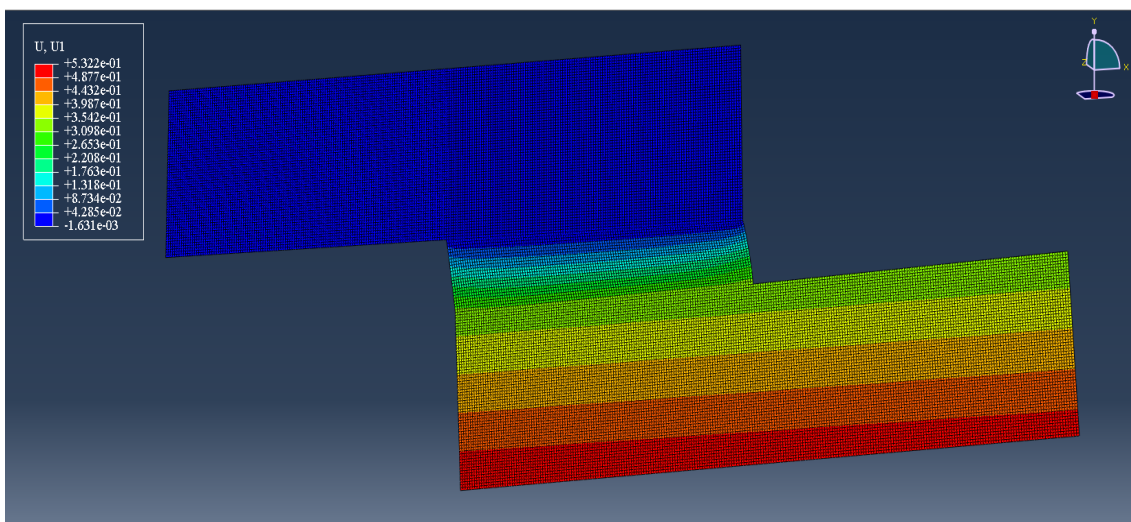


Fig. 11. Contour of displacement component u_1 for adhesive I

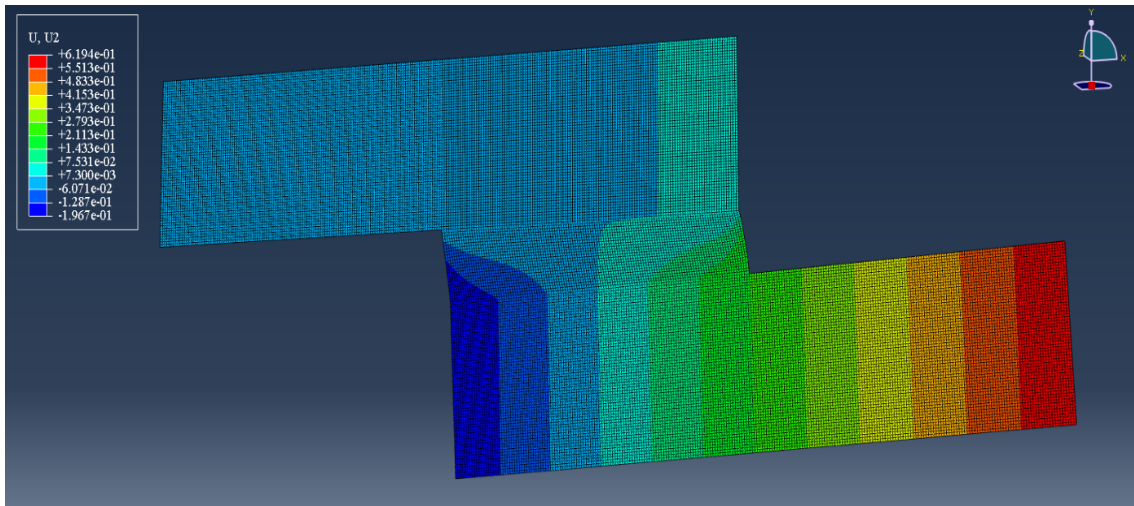


Fig. 12. Contour of displacement component u_2 for adhesive I

Figure 11 and 12 show the contour of axial and transverse displacement respectively. Maximum displacement occurs near lower adherend where the load is applied. The transverse displacement is greater than the axial displacement. Large stress and displacement occur near the edge region. Delamination and failure may occur due to large displacement and stress concentration. Therefore, selecting a proper adhesive to reduce the chance of failure is very important.

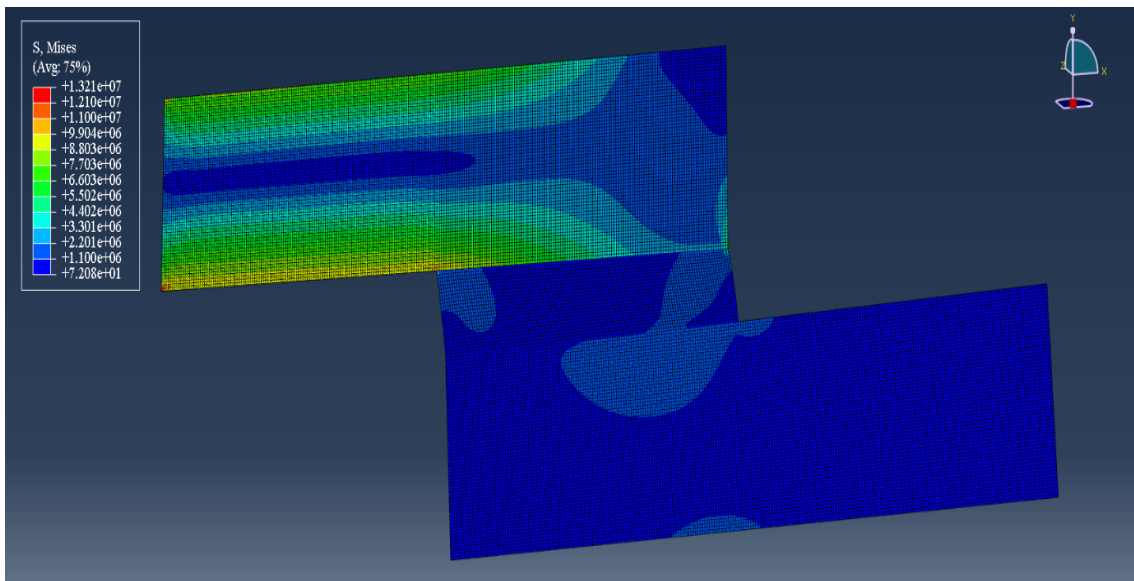


Fig. 13. Contour of Von Mises stress for adhesive I

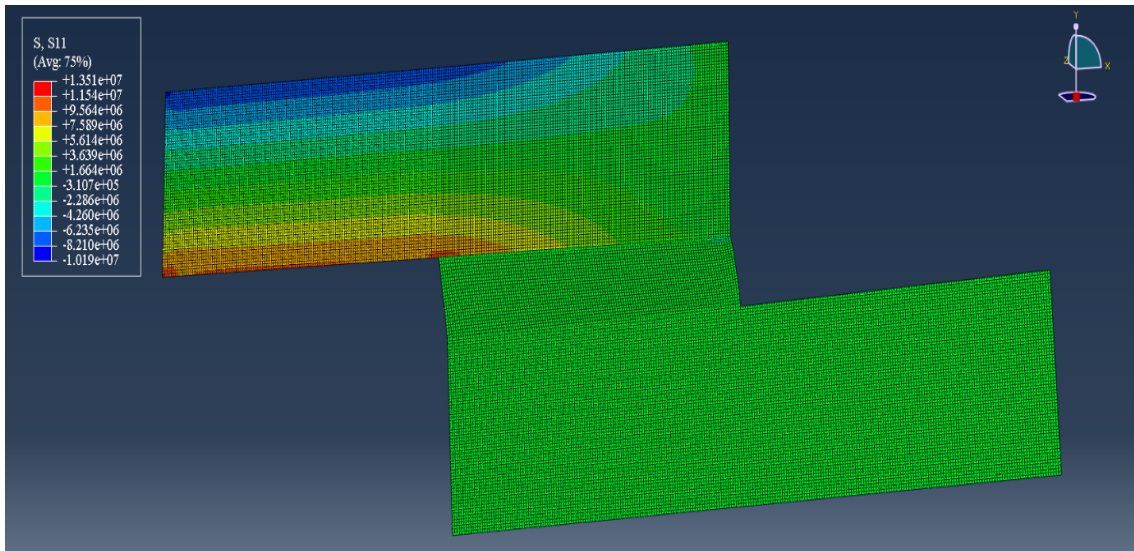


Fig. 14. Contour of stress component σ_{11} for adhesive I

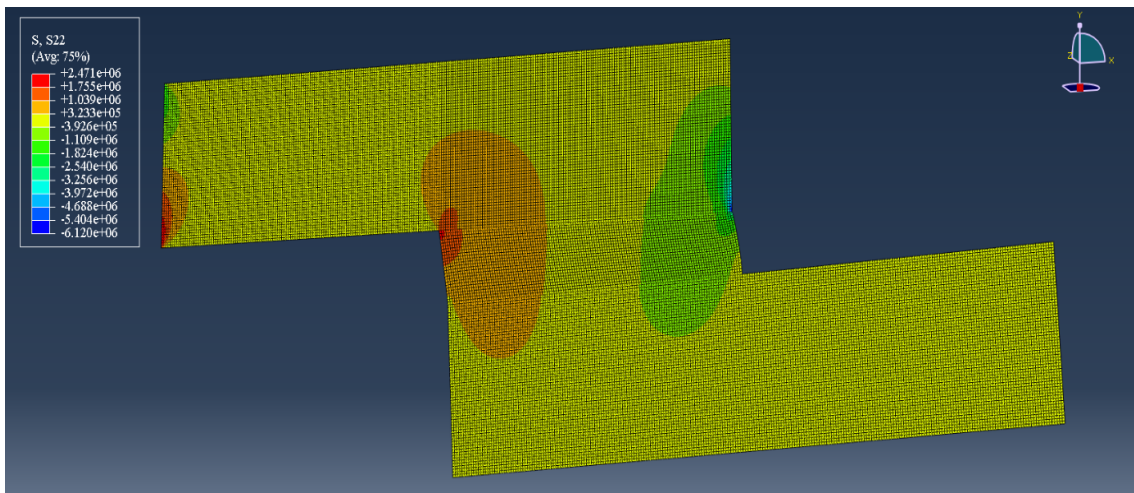


Fig. 15. Contour of displacement elements σ_{22} for adhesive I

Figure 13,14 and 15 show the contour of Von Mises stress, σ_{11} and σ_{22} respectively. Maximum stress occurs near the interface region than the other regions. Stress is found to be maximum near the edge due to the occurrence of stress singularity near the singular point. As the Modulus of elasticity and poisson ratio of adhesive decreases singular stress also decrease. Due to high stress concertation delamination may occur. Therefore, selecting proper adhesive is important to reduce the chance of failure.

7. Conclusions

Using a commercial 2-D finite element code, the effect of adhesive characteristics on the interfacial stress field of adhesively bonded joints was examined. For five types of adhesive, the stress distributions along the bond length of adhesive-bonded joints are determined. The

results indicate that Young's modulus and Poisson's ratio have a significant impact on the stress and displacement fields of an adhesively bonded joint. In addition, the research reveals that the adhesive-bonded joint's strength can be increased by selecting an adequate adhesive. By analyzing five different models it can be concluded that adhesive I should be utilized for operation.

Acknowledgments

The authors would like to thank GOD for His enormous grace in allowing them to conclude their research.

Notations

u_i	Nodal displacements
ψ_i	Lagrange interpolation function
E	Young's Module
ϕ_i	Hermit interpolation function
$\{\Delta\}$	Nodal displacement vector
$\{F\}$	Nodal force vector

References

- [1] Liao L., Sawa T., Huang C., Numerical analysis on load-bearing capacity and damage of double scarf adhesive joints subjected to combined loadings of tension and bending. *International Journal of Adhesion and Adhesives*, 53, 65–71, 2014.
- [2] Methfessel, T. S., Becker, W., A generalized model for predicting stress distributions in thick adhesive joints using a higher-order displacement approach, *Composite Structure*, 291, 2022.
- [3] Somadder, S., Islam S. Md., Effect of Adhesive Layer Thickness and Slant Angle on Piezoelectric Bonded Joints, *Journal of Mechanical Engineering*, 19, 251-268, 2022.
- [4] Tsai M.Y., Oplinger D.W., Morton J., Improved theoretical solutions for adhesive lap joints, *International Journal of Solids and Structures*, 35, 1163–1185, 1998.
- [5] Mokhtari M., Madani K., Belhouari M., Touzain S., Feugas X., Ratwani M., Effects of composite adherend properties on stresses in double lap bonded joints, *Materials and Design*, 44, 633–639, 2013.
- [6] Moya-Sanz E.M., Ivañez I., Garcia-Castillo S.K., Effect of the geometry in the strength of single-lap adhesive joints of composite laminates under uniaxial tensile load. *International Journal of Adhesion and Adhesives*, 72, 23–29, 2017.

- [7] Ozel A., Yazici B., Akpinar S., Aydin M.D., Temiz S., A study on the strength of adhesively bonded joints with different adherends, *Composites Part B: Engineering*, 62, 167–174, 2014.
- [8] He X., Gu F., Ball A., Fatigue Behaviour of Fastening Joints of Sheet Materials and Finite Element Analysis, *Advances in Mechanical Engineering*, 5, 1-9, 2013.
- [9] Zhao L., Wang Y., Qin T., Zhang J., X., A New Material Model for 2D FE Analysis of Adhesively Bonded Composite Joints, *MATERIALS SCIENCE*, 20, 468-473, 2014.
- [10] Pires I., Quintino L., Miranda M. R., Numerical simulation of mono- and biadhesive aluminium lap joint, *Advances in Mechanical Engineering, Journal of Adhesion Science and Technology*, 20, 19-36, 2006.
- [11] Rodríguez Q. R., Sollero P., Rodrigues B. M., STRESS ANALYSIS AND FAILURE CRITERIA OF ADHESIVE BONDED SINGLE LAP JOINTS, 21st International Congress of Mechanical Engineering, 2011.
- [12] He X., Dynamic Behaviour of Single Lap-Jointed Cantilevered Beams, *Key Engineering Materials*, 413, 733-740, 2009
- [13] He X., Zhang Y., Numerical Studies on Mechanical Behavior of Adhesive Joints, *Advances in Materials Science and Engineering*, 2015, 1-13, 2015.
- [14] Ozer H., Oz O., Three dimensional finite element analysis of bi-adhesively bonded double lap joint, *International Journal of Adhesion and Adhesives*, 37, 50-55, 2012.
- [15] He X., Wang Y., Analytical Model for Predicting the Stress Distributions within Single-Lap Adhesively Bonded Beams, *Advances in Materials Science and Engineering*, 2014, 1-5, 2014.
- [16] Andruet H. R., Dillard, A. D., Holzer M. S., Two- and three-dimensional geometrical nonlinear Finite elements for analysis of adhesive joints, *International Journal of Adhesion and Adhesives*, 21, 17–34, 2001.
- [17] Koguchi H., Costa D. A. J., “Analysis of the stress singular field at a vertex in 3D bonded structures having a slanted surface,” *International Journal of Solids and Structures*, 47, 3131-3140, 2010.
- [18] He X., “Effect of Mechanical Properties of Adhesives on Stress Distributions in Structural Bonded Joints” *World Congress on Engineering*, 2010.